INTEGRATION OF GEOREFERENCED INFORMED SYSTEM AND DIGITAL IMAGE ANALYSIS TO ASSES THE EFFECT OF CARS POLLUTION ON HISTORICAL CITIES.

R. Ortiz*[a], P. Ortiz[a], M.A. Vázquez[b], J.M. Martín[a]

[a]Universidad Pablo de Olavide, Department of Physical, Chemical and Natural Systems. Carretera de Utrera Km 1, ES-41013 Sevilla, España

[b] Department of Crystallography, Mineralogy and Q.A., Calle Profesor García González, S/N, ES- 41072 Sevilla, España

* Corresponding author: Rocío Ortiz

E-mail: rortcal@upo.es

ABSTRACT

The blackening of monuments in historic cities due to air pollution is common. In historic urban centres, pollution from traffic negatively affects the preservation of monuments and results in the appearance of black crusts and/or deposits. The cleaning procedures for restoring or rehabilitating these building to remove these deposits are expensive and require continuous effort. Thus, it is necessary to monitor and control the effects of traffic on buildings. The objective of this study was to develop a new analytical methodology to assess and evaluate the continued risk of traffic pollution due to the circulation of vehicles near monument facades. This methodology combines geographic information systems (GIS) and digital image analysis (DIA) to evaluate the effect of traffic on the facades of stone buildings, which will enable more informed decisions regarding the reorganisation of traffic and the pedestrianisation of streets near monuments.

Keywords: pollution, blackening, traffic, georeferenced system, digital image analysis, monuments.

1. Introduction.

The current developmental model of society has resulted in large cities with increasing numbers of vehicles and industrial zones. Due to air pollution, many monuments and historic buildings have begun to deteriorate [1-2].

Motor vehicles are the largest source of air pollution in urban areas. Carbon monoxide (CO) is the most common pollutant emitted by vehicles. Vehicles are also a significant source of particulate emissions, NOx, and SO_2. The negative effects of air pollution on the building materials of monuments are well-known; particles may accumulate on the building surface, affecting its outward aspect, in addition to chemical reactions of pollutants with building materials [3]. Deposits and crusts on buildings are basically generated by two phenomena: dry and wet deposition. In dry deposition, pollutants adhere directly to the stone surface. In wet deposition, blackening is produced by oxidation in the presence of gas or solid catalysers, such as SO_2 and NO_x, resulting in the formation of different acids (principally H_2SO_4 and HNO_3) that begin to dissolve the stone surface. This phenomenon occurs extensively with materials composed of carbonates, such as marble, limestone, and calcarenite. Several investigations have been completed on the impact of air pollution on cultural heritage [4-6] and the appearance of mechanical damage [7] or black crust due to traffic and atmospheric SO_2 [8-9]. These studies demonstrate that walls directly exposed to traffic have higher concentrations of sulphate, nitrate, and organic carbon.

The damage layers in blackening and black crust [6] are a record of the environmental changes over time, and some differences in thickness exist [10] from different exposures to vehicular traffic.

Black crusts generated by pollution should be periodically removed from buildings using lasers, superficial cleaning, pressure washing, or chemical products, which may tangibly or intangibly damage these sites of historical significance. The expense associated with these restoration projects varies based on the costs of amortization of the instrumentation, consumable products required for cleaning, and operation time [11]. The costs are already high and must be incurred periodically in cities due to increases in pollution.

For these reasons, European legislation has been concerned with the effects of air quality on populations, ecosystems and, more recently, cultural heritage. Regarding risk assessment and the vulnerability of historical buildings to pollution, the basic texts of the Council of Europe [12] explicitly address physical deterioration due to pollution and refer to risks as the damages or foreseeable losses of cultural heritage that are caused by deterioration and accentuated by pollution and poor preservation. As in many developed countries, legislation in Spain addresses the exposure of historical buildings to pollutants as one of the factors guiding the establishment of air quality objectives and alert thresholds [13]. However, analysis of the actual risk of pollution in the environment and evaluation of the damages to historical buildings are rare.

In the cities and historical centres of Spain, local governments have jurisdiction in measures relating to urban traffic and are included in air quality improvement plans under Decree 239/2011 [14], by which the quality of atmospheric air is regulated. In this decree, a classification of traffic levels as a function of number of vehicles is found. A high volume of traffic represents more than 10,000 vehicles/day, medium volume represents between 3,000 and 10,000 vehicles/day, and low volume represents between 500 and 3,000 vehicles/day. The aforementioned decree is also connected to the guidelines established in

Directive 2008/50/CE [15] to promote better environmental air quality and a cleaner atmosphere for Europe.

One of the guidelines for action in the National Plan of Climate Change Adaptation (Plan Nacional de Adaptación al Cambio Climático) [16] contemplates the evaluation of the potential impacts of climate change on cultural heritage (tangible or intangible) and its repercussions for tourism. However, no defined methodology exists for analysing the effects of air pollution on historical centres or on sites destined for preservation. For this reason, a new methodology is proposed in this article to combine geographic information systems (GIS) and digital image analysis (DIA) at the street level, considering sources of pollution, the flow of traffic, and the dispersion of pollutants, as well as the geographical location of monuments in the historical centre.

GIS is a tool used in different fields, such as in architectural inventories of rammed earth construction projects, which include the historical context, topographical data, and architectural characteristics and details of buildings [17], studies of rural construction projects [18], hazard evaluations [19] integrated with satellite remote sensing systems to assess flood risks [20-22], and in combination with RAMAN and SEM-EDX to study the pollutants on walls [23].

DIA may be combined with other techniques or used on its own, and it represents a useful methodology for the identification of different types of materials [24-26], weathering forms [27], signs, and drawings [28-30] or lichens, as well as for the analysis of the effectiveness of biocides [31] or the study of black crusts that have formed on buildings [32-33]. As a complement to other techniques, DIA is a non-destructive technique that also serves to evaluate salt damp on walls [34-35] and provides detailed materials mapping for the evaluation of the compatibility of conservation interventions [36]. In combination with remote sensing techniques, DIA of mural paintings allows for an understanding of the interactions of the different elements in a system that has diverse spatial positions [37]. Thus, this method is extensive and has several applications, and its results may guide decisions concerning the rehabilitation, cleaning, and consolidation of historical buildings. For these reasons, this method was selected to quantify damage to stone facades due to air pollution.

2. Methods

2.1. Study area

To demonstrate the application of the methodology, the city of Seville in the southern Spain was selected. The study area is approximately 3.7 km2, and 13 facades of the most emblematic and ancient monuments were considered (Table 1). These parishes were built in the Gothic-Mudejar, Renaissance, and Baroque styles between the XIIIth and XVIIIth century.

Table 1. Individual buildings chosen for study in the historic centre of Seville and the district of Triana, along with code, periods of construction, architectural style, number of samples taken and number of facades studied by digital image analysis. Note: The churches with digital image analysis studies are shaded.

Church (Code)	Period of Construction	Architectural Style	No. of samples	No. facades Digital Image Analysis	Façade Orientation
La Anunciación (ANUN)	16^{th} Century (1565-1579)	Renaissance	11	1	North

La Magdalena (MAG)	17^{th}-18^{th} Century (1691-1709)	Baroque	11	1	South-East
Omnium Sanctorum (OS)	13^{th} Century (1250-1399)	Gothic-Mudejar	14	3	North West South
San Esteban (SES)	14^{th}-15^{th} Century (1349-1414)	Gothic-Mudejar	8	Not enough distance to take a complete photo	
San Gil (SGI)	14^{th} Century (1300-1399)	Gothic-Mudejar	6	Recently restored	
San Ildefonso (SIL)	18^{th}-19^{th} Century (1794-1841)	Neoclassical	8	No stone in the facade	
San Isidoro (SISI)	14^{th} Century (1345-1354)	Gothic-Mudejar	5	Recently restored	
San José (SJO)	18^{th} Century	Baroque	4	Not enough distance to take a complete photo	
San Juan de la Palma (SJP)	15^{th} Century (1400-1499)	Gothic-Mudejar	7	Not enough distance to take a complete photo	
San Julián (SJU)	14^{th}-15^{th} Century7 (1300-1407)	Gothic-Mudejar	4	1	West
San Lorenzo (SLO)	14^{th} Century (1300-1399)	Gothic-Mudejar	4	2	North South
San Marcos (SMARC)	14^{th} Century (1345-1354)	Gothic-Mudejar	9	Not enough distance to take a complete photo	
San Martín (SMTIN)	15^{th} Century (1400-1432)	Gothic-Mudejar	7	1	West
San Nicolás (SNIC)	18^{th} Century (1758-1799)	Baroque	11	1	South
San Pedro (SPE)	15^{th} Century (1440-1499)	Gothic-Mudejar	10	1	South
Santa Ana (Triana) (STA)	13^{th}-14^{th} Century (1285-1350)	Gothic-Mudejar	5	Recently restored	
Santa Catalina	14^{th} Century (1350-	Gothic-Mudejar	12	1	West

(STCA)	1399)				
Santa Cruz (STCR)	17th-18th Century (1665-1728)	Baroque	14	1	North-West
Santa Inés (STIN)	14th Century (1374)	Gothic-Mudejar	7	Recently restored	
Santa Isabel (STIS)	17th Century (1602-1699)	Baroque	4	1	South
Santa Marina (STMA)	14th Century (1356)	Gothic-Mudejar	11	1	West
Santa María la Blanca (STMB)	17th Century (1650-1665)	Baroque	6	Recently restored	
San Román (SRO)	14th Century (1356-1399)	Gothic-Mudejar	2	Recently restored	
San Vicente (SVI)	14th-16th Century (1300-1599).	Gothic-Mudejar	8	1	South
El Salvador (SALV)	17th-18th Century (1674-1712)	Baroque	2	Recently restored	
San Andrés (SAND)	14th Century (1300-1399)	Gothic-Mudejar	2	Recently restored	
Santiago (SANT)	14th-18th Century	Gothic-Mudejar	3	No stone in the facade	
San Bartolomé (SBAR)	18th Century (1780-1796)	Neoclassical	2	Not enough distance to take a complete photo	
Sagrario (SAG) (Catedral)	17th Century (1618-1622)	Baroque	6	1	West
La O (Triana) (O)	17th-18th Century (1697-1702)	Baroque	2	Recently restored	

2.2. Study of weathering forms on the facades of monuments

The weathering forms were studied to establish the effects of pollution on the facades of monuments using the visual inspection, following ICOMOS-ISCS [38]. Otherwise, samples of black crusts and deposits were taken from the facades of the buildings at different heights (Table 1). The sampling followed the recommendations of the technical commission CNR-ICR NORMAL 3/80 [39].

To characterise the black crusts and deposits on church facades, the following techniques were used:

a) The black crusts and/or deposits of samples were described with the aid of a ZARBECO 2000 magnifying lens. The front and back surfaces of the samples were viewed under visible, ultraviolet, and infrared light. A cut perpendicular to the surface was viewed with a KYOWA transmitted light petrographic microscope attached to a digital camera, a Leica 5400 LV optical microscope attached to a digital camera, and a JEOL JSM‐5400 scanning electron microscope with energy dispersive x-ray spectroscopy (SEM-EDX).

b) The building materials and the content of newly formed crusts and deposits were characterised using x-ray diffraction with a Bruker model D8C system and x-ray fluorescence using PANalytical Axios and Epsilon 5 spectrometers.

c) For samples from facades with different degrees of alteration, the rate of blackening and the thickness of the crusts and/or deposits was evaluated with a ZARBECO 2000 magnifying lens, and the digital analysis of images was completed for a 4 mm2 surface area.

2.3. Using a Geographic Information System (GIS) to build a map of pollution

ArcGIS was employed to evaluate the traffic of vehicles on all streets in the centre of Seville (Spain).

Air pollution data were provided by the Environmental Information Network of the Council of Andalucia (Red de información Ambiental de la Junta de Andalucía; REDIAM) was consulted [40] for measurement stations at different points in the city, including the historic centre, La Ranilla, Príncipes, Torneo, and Santa Clara (figure 1). The only stations located inside the historical district were located on the streets of Pajaritos and Torneo; these have low and very high levels of traffic, respectively.

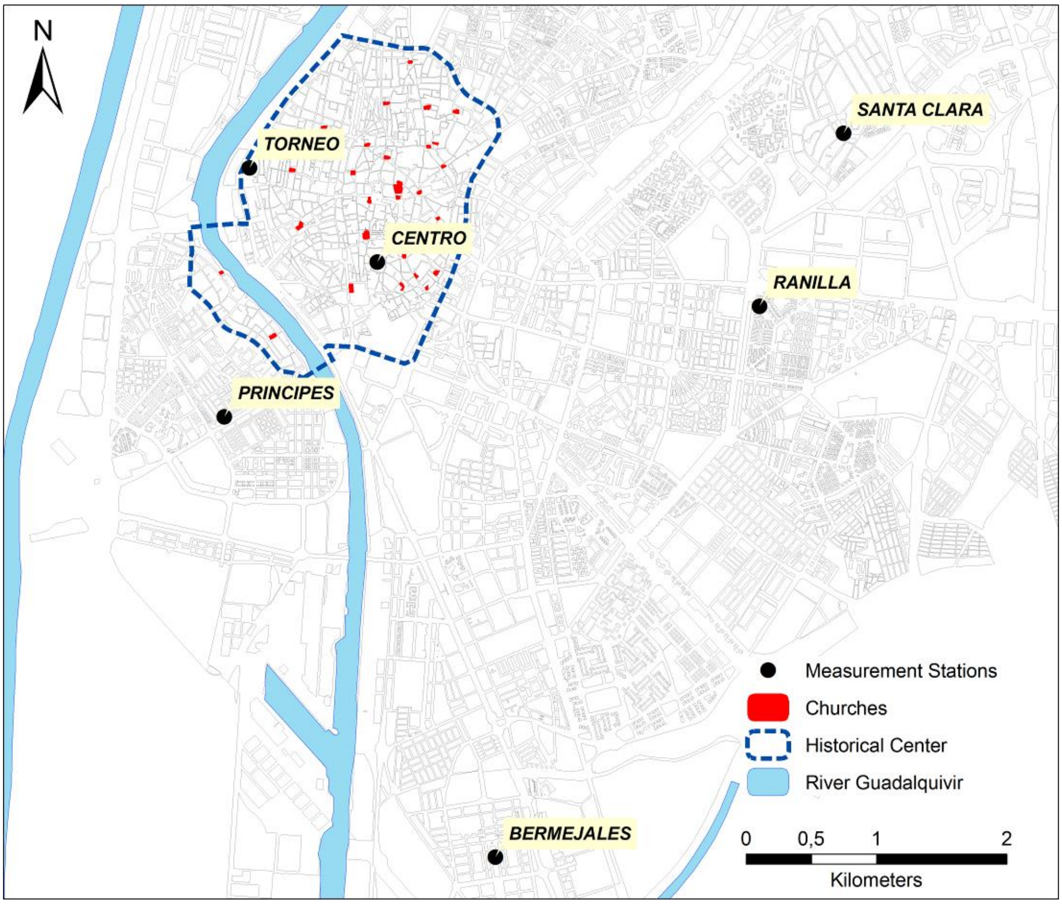

Figure 1. Location of churches studied and measurment stations in Seville (Spain).

Four atmospheric pollutants and their potential effects on the historical buildings of the city were analysed for 1999–2015: sulphur dioxide (SO_2), suspended particulate matter with a diameter ≤ 10 µm (PM10), carbon monoxide (CO), and nitrogen oxide (NO_x).

In addition, potential point sources of pollution, such as circulating traffic and industry, were analysed, as was street width, which could affect the dispersion of pollutants from traffic. Table 2 provides details on the criteria used to classify risk; each historic building was assigned a value of 1 to 5 from least to most hazardous, as a function of the average daily level of traffic and the street width.

The General Urban Plan of Seville (Plan General de Ordenación Urbanística de Seville; PGOU) [41] revealed that the average daily levels of traffic (vehicles/day) for the main circulation routes of the historic centre are between 40,000 and 120,000 vehicles/day in the southern zone and between 25,000 and 40,000 vehicles/day along the main northern road. The level of traffic on the entrance and exit ways to the city varies from 0 to 8,000 vehicles/day. According to Decree 239/2011, the traffic level is considered high for the entire loop if it surpasses 10,000 vehicles/day, and for routes accessing the historical centre, between 3,000 and 10,000 vehicles/day.

During business days, the traffic on the access roads to the historic centre, the streets Aguilas and Puerta de la Barqueta, surpasses 800 vehicles/hour. The exit ways, the streets San Luis and Santa Maria la Blanca, have an approximate volume of 400 vehicles/hour [42]. These data were used to assess the hazard to nearby historic monuments due to circulating traffic.

The street width also influences the appearance of black crusts [43]; for streets with a width of less than 5 m, the hazard factor was increased by 1 unit. This analysis was performed using data from the Virtual Land Registry Office (Oficina Virtual del Catastro) [44], which were provided in a geographic information system, to calculate the distance between blocks.

Table 2. Classification of streets according to traffic level and street width.

Criteria	Hazard	Intensity					
		+/-	1	2	3	4	5
			Very low	Low	Moderate	High	Very high
1	Traffic roads	-	Pedestrian	Others	Roads with public transport	Access to the historic centre and exit ways	Loop
2	Street width < 5m	-	+1 level in traffic roads	+1 level in traffic roads	+1 level in traffic roads	+1 level in traffic roads	

2.4. Digital image analysis

Maps created with computer aided design (CAD) from previous studies of the facades of the Santa Cruz and Omnium Sanctorum churches [45-46] demonstrate the relationship between the extension of black crusts/deposits and traffic intensity; however, this technique could not easily evaluate the thickness of the deposits or the degree of blackening of the facades. The DIA methodology was developed by [47] based on the examples of [34-35] to study the thickness of the weathering forms on walls, following a series of logical operations to segment and separate images by sets of pixels.

The methodology detailed below was performed with colour images of 13 church facades in the historical centre of Seville (Table 1). First, the colour images were converted to black and white. Then, a histogram of the distribution of grey levels for each image was obtained, where different levels represented the main alteration typologies present on the facades.

a) Level segmentation and quantification of images

To create a map of damage and to establish the different levels of stone alteration, the image was segmented at several levels. For this, a comprehensive spectral survey was performed for each image to identify the range of grey levels, which corresponded to different alteration typologies. With upper and lower thresholds of zero and 255, respectively, four cut-offs were established, enabling the image to be classified into one of five categories. In this way, the multi-valued images were processed, and well-preserved stone could be distinguished from altered stone, whether uncovered or covered by black crusts of varying thicknesses.

To improve visualisation, a colour palette with five colours was created; three colours were assigned to stone with a distinct thickness of black deposits, ordered from greater to lesser thickness (blue, green and yellow). One colour was assigned to stone without deposits (white), and the colour red indicates a loss of the material or building works. Finally, the colour black represents areas that are not stone, such as doors and windows.

b) Binarisation and quantification of images

The spectral surveys of the images may also be classified by the threshold or binarisation technique into two distinct categories: 1) areas of stone and 2) areas with material loss and/or alveolization. This technique is used to distinguish chromatic alterations or discolourations from the rest of the stone.

An algorithm was used to segment the image into two groups, by converting the 256 grey levels of the image into only two populations. A threshold was calculated for the histogram for the number of thresholds, n = 1, with the number of populations expressed by n + 1 = 2. The grey level for each threshold varied by image. In the resulting binary image, pixels with higher levels of grey were assigned a value of 1, corresponding to the loss of material or chromatic alterations, and the remaining pixels with grey levels less than the threshold were assigned a value of 0, separating the rest of the structure.

Once this new categorisation was obtained, the digitalised image was superimposed on the image of the previous section (Section a).

Then, the percentages of the distinct populations obtained in the images of each facade were calculated, first subtracting the pixels corresponding to the black palette of the superimposed image to exclude areas that do not represent stone.

3. Results and discussion

3.1 Study of weathering forms on the facades of monuments

The predominant materials used in the thirty facades of the monuments studied in Seville were bricks, calcarenites, limestones, mortars, and marbles [43, 48]. The most common weathering forms on the buildings of the study were missing parts, colouration, discolouration, moist area, soiling, efflorescence, black crust, cracking, fracturing, sanding, detachment, biological colonisation, plants, and building works.

Figure 2 shows the analysis of the thirteen weathering forms more frequently taking into account traffic roads criteria (table 2).

In Figure 2, a direct relationship is observed between the level of traffic and the weathering form by black deposits. Streets with very high levels of traffic were excluded because no monuments were found on these roadways. For streets with high or medium levels of motorised vehicle traffic, deposits are present on 94 and 62 % of the facades, respectively, whereas for facades on streets with low vehicle transit, the presence of deposits decreases considerably (< 45 %). Approximately 60 % of monuments on streets with medium levels of traffic exhibited deposits, which is relatively higher than what would be expected, likely due to the influence of narrow streets because vehicles circulate in closer vicinity to the facades; however, the incidence of deposits may also depend on the time since the last restoration.

Black crusts are plainly visible and may be observed more easily on streets with a high density of circulating traffic and on narrow streets where traffic circulates in closer proximity to the facades.

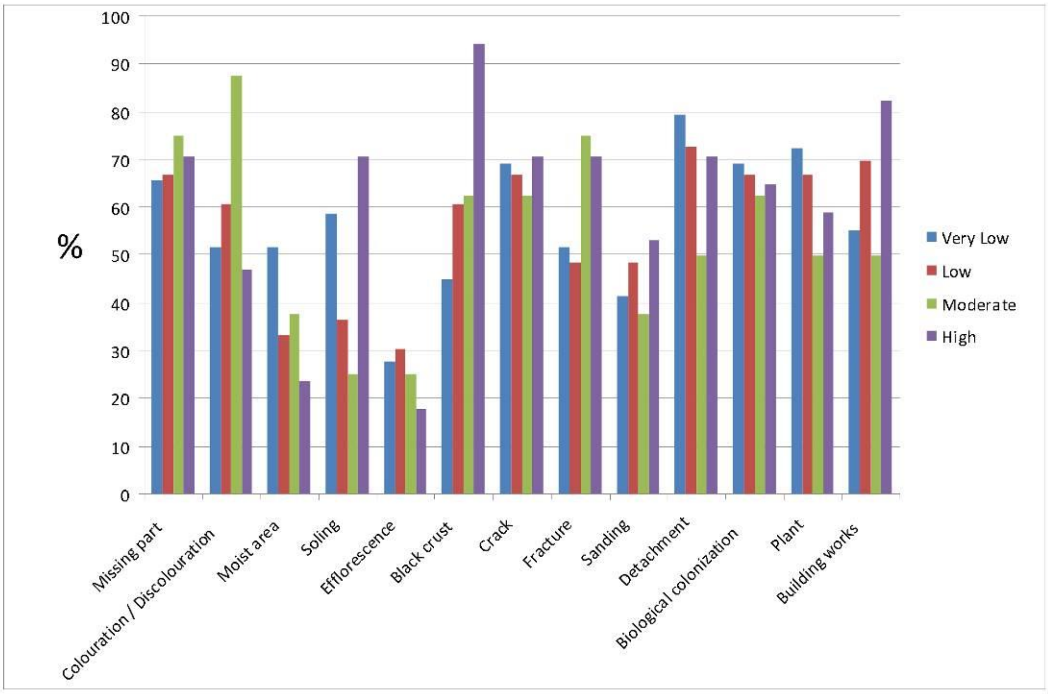

Figure 2. Frequency of weathering forms at the studied churches according to level of traffic.

The mineralogical characterisation by x-ray diffraction of the deposits and black crust samples from the studied buildings revealed the presence of gypsum ($CaSO_4.2H_2O$) in 40 of the samples. This sulphate was mostly discovered as part of black crusts but was also found sporadically (< 2 %) due to the disintegration of surrounding mortar or other repairs associated with the deposits.

The chemical analysis of crusts and deposits was also assessed by x-ray fluorescence (XRF; Figure 3). Calcium oxide (CaO) was found at high concentrations by XRF and formed a major component in 75 % of the samples; this compound is associated with calcite in rocks and mortars. The silicon content varied by sample, according to the nature of the construction material, with higher values corresponding to mortars. The CaO content associated with losses due to calcination implies that the majority of samples have a high level of calcium, which is in agreement with the XRF results from construction materials. This predominant chemical-mineralogical composition of the building materials of the architectural heritage of Seville implies high vulnerability to air contaminated with sulphur and nitrogen oxides under the local meteorological conditions [49]. In this case, calcite also tends to react easily with atmospheric sulphur oxides to form gypsum on the building surface, generating a black crust. Of the 90 samples of crusts and deposits analysed by XRF, more than 80 % had SO2 content above 1 % (Figure 3), which is considered to be a high level of sulphur because the samples analysed from the quarry do not contain this component at all or it appears in quantities of less than 0.05 %. This percentage of samples with SO_2 confirms the formation of gypsum ($CaSO_4.2H_2O$) to be a consequence of the reaction of the calcium carbonates of the facade materials with polluting sulphur gases in the environment. In 75 % of the samples, this alteration is associated with a sulphur oxide content greater than 1 % W/W, whereas the remaining portion is due to the alteration of joints, repositioning of mortars or the capillary ascension of moisture.

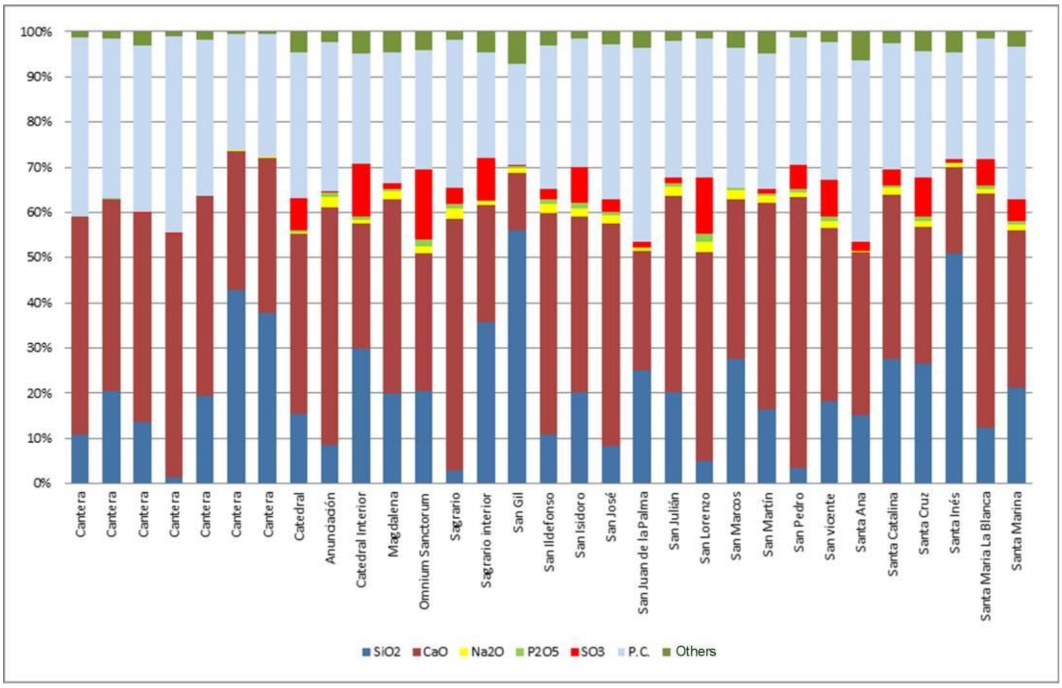

Figure 3. Chemical composition analysis of crusts and deposits determined via x-ray in comparison with samples of quarries. (Percentage %W/W). Note: PC corresponds with loss due to calcination.

According to Bromblet and Verges-Belmin [50], to perform a more detailed analysis of the processes surrounding the formation of crusts and deposits, their microtexture must be identified. For this reason, a petrographic study of thin films taken perpendicular to the surface material was performed using a scanning electronic microscope with energy dispersive spectroscopy (SEM-EDX), in which the stratigraphy of the deposits and crusts were prepared and embedded in methacrylate.

Of the 44 thin films studied, deposits and/or black crusts were observed in samples from the churches of San José, Santa Catalina, San Pedro, Santa Cruz, San Nicolás, Omnium Sanctorum, Santa María La Blanca, and Sagrario

(Cathedral). The second facade of the San José church faces a street classified as very high risk due to the circulation of traffic because it is located on the exit way of the historic centre, with a street width of less than 5 m. Santa Catalina, San Pedro, Santa Cruz, Omnium Sanctorum and Santa María la Blanca are considered at risk due to high levels of traffic as they are located on the exit or entry ways to the centre, although their corresponding streets are wider than 5 m. San Nicolás is located on a street with a medium level of traffic, whereas Sagrario (Cathedral) is situated near streets with low or very low levels of traffic. The streets surrounding Sagrario (Cathedral) previously formed part of the main entrance ways to the city centre for public and private traffic, until the traffic reorganisation of 2009, when street traffic in this area was modified to pedestrian-only.

Crust and deposit sections perpendicular to the studied surface were analysed using a scanning electron microscope coupled with energy dispersive spectroscopy [43]; more than 120 samples were considered, of which 80 % contained sulphur and calcium, indicating chemical reactions with sulphur oxides from the atmosphere. The crust layers varied in thickness from 20–1000 μm. Figure 4 shows the image of the black crust found on the Santa Cruz church, in which sulphur and calcium were detected in the exterior layer by SEM-EDX (Figures 4B and D). Above the layer of gypsum, particles and compounds that generate the black colour of the crust accumulate (Figure 4A shows the cross-section, and Figure C shows the parallel cut).

Based on the degree of alteration, crusts may be classified as fine, intermediate or high thickness using DIA (Figure 5). The histograms of the digital images shift as a function of the degree of alteration. In Figure 5, several samples from the Santa Catalina church with varying levels of crust may be observed. In Figure 5A, the histogram shits towards the right, indicating higher levels of white and fewer deposits, and when the surface is covered with intermediate levels of crust (Figure 5B), the histogram is centred. Finally, for the most altered samples with the highest levels of deposits (Figure 5C), the histogram is shifted to the left. This displacement of the histogram values obtained by DIA allows us to view the different stages of the formation of black crusts and/or deposits, from beginning to advanced.

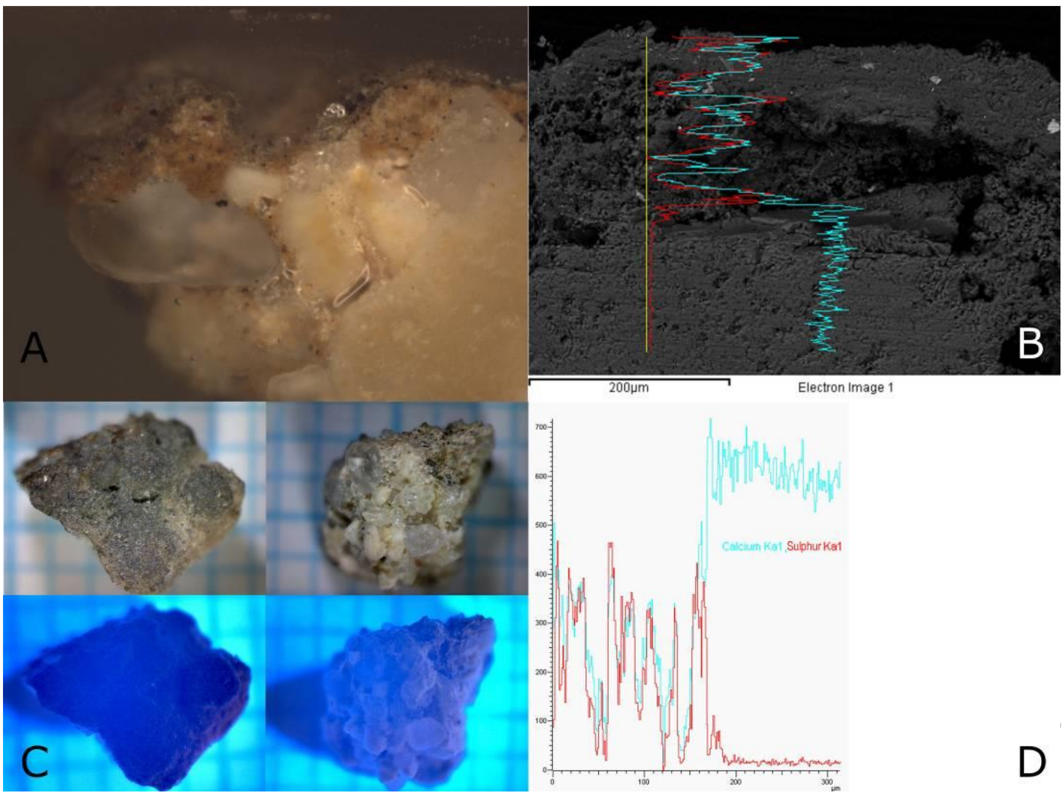

Figure 4. A) Stratigraphy of sample from Santa Cruz church viewed with an optical microscope; black and brown deposits are visible, with a thickness range of 150–300 µm. B and D) Scanning electron microscope image coupled with energy dispersive spectroscopy; visible layers of sulphur and calcium are detected on the surface. C) Magnified images under visible and ultraviolet light of the front and back of a crust sample (scale = 1 mm); the extent of blackening may be observed.

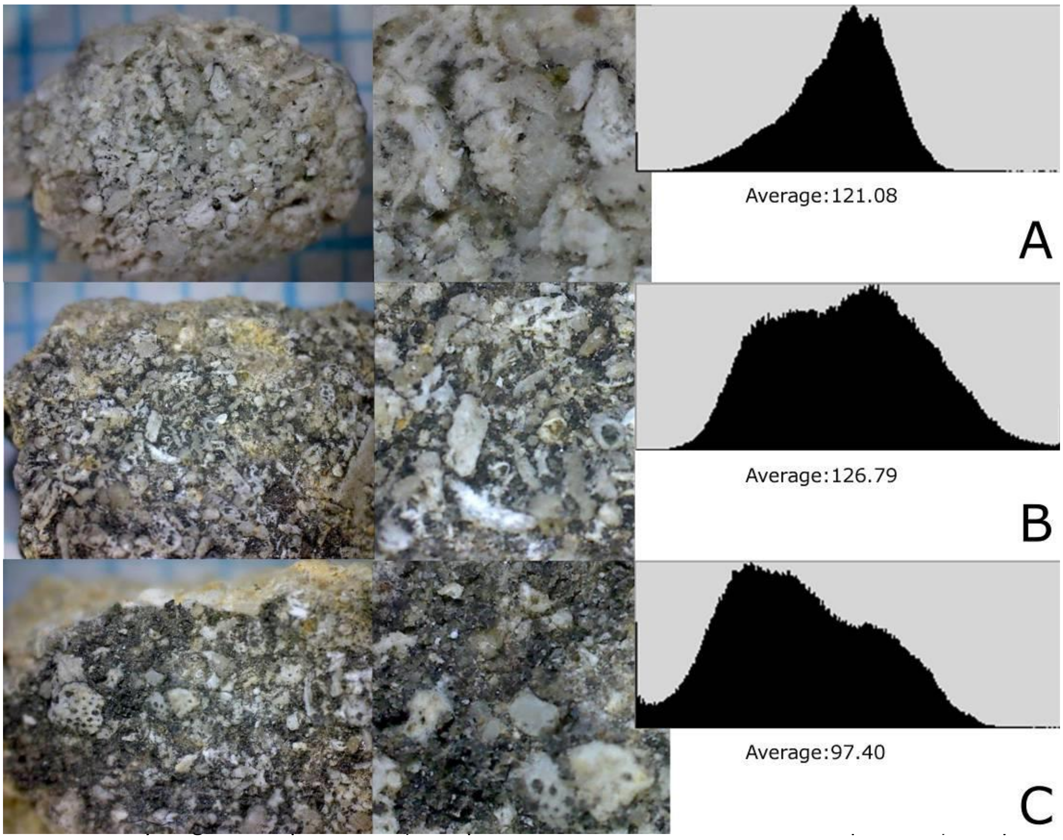

with extensive deposits.

3.2. Pollution hazard map created using GIS

The city of Seville, located in a small depression of the Guadalquivir Valley, is surrounded by several landforms (Aljarafe to the west and Alcores to the east), and the Guadalquivir River crosses the city from north to south; this basin is characterised by the phenomenon of thermal inversion, which causes diffusion and dispersal of emitted air to be difficult [51]. In Seville, industrial anthropogenic emissions are quite low, with the main pollution source being vehicular traffic [52-53].

Of the chemical pollutants present in the atmosphere of Seville, five have been studied using REDIAM data [40] to relate their presence with the circulation of traffic or with damages to historical buildings. Table 3 shows the annual averages of the air pollutants, including nitrogen oxides (NO_X), sulphur dioxide (SO_2), ozone (O_3), particulate matter ≤ 10 µm (PM10), and carbon monoxide (CO).

Table 3. Pollution data of CO, NO_x, O_3, PM_{10}, SO_2 (µg/m³). Measurment stations of Bermejales, Centro, Principes, Ranilla, Santa Clara y Torneo.Data from REDIAM [40].

	µg/m³	1999	2001	2002	2003	2004	2005	2006	2007	2008	2009	2010	2011	2012	2013	2014	2015
BERMEJALES	**CO**													457,58	460,22	373,88	662,78
	NO_X													41,42	39,41	45,22	53,29
	O_3													51,40	56,82	54,90	54,11
	PM_{10}													32,66	28,03	23,81	35,04
	SO_2													5,03	4,90	5,15	5,10
CENTRO	**CO**				333,55			413,81	463,80	506,84	476,54	516,70	744,51	721,40	685,20	474,90	483,00
	NO_X						53,57	40,59	38,14	34,09	35,47	39,88	36,91	33,00	32,80	29,50	37,00
	O_3					45,79	49,86	50,14	50,84	52,67	53,89	55,61	55,68	52,20	57,40	55,90	54,00
	SO_2				3,60	6,71	4,08	1,62	1,96	3,56	2,27	2,63	3,11	2,70	3,10	3,10	3,00
	PM_{10}				33,81												
PRINCIPES	**CO**	1016,57	996,35		955,19	1201,13	868,41	619,63	601,88	534,76	481,47	428,97	413,83	415,34	389,28	341,64	472,54
	NO_X	73,48	72,48		62,87	57,82	75,67	63,20	64,88	63,21		42,21	53,53	48,00	42,46	39,08	45,85
	PM_{10}	41,31	38,50		33,62	35,27						30,61	31,46	28,95	25,26	26,10	30,41
	SO_2	7,06	7,53		6,95	8,53	12,27	6,20	6,16	7,88	5,20	5,80	6,22	5,20	6,20	7,63	9,32
RANILLA	**CO**	1666,20	1360,14	1259,88	1122,39	1032,37	1043,25	711,28	695,29	644,25	613,77	650,77	270,25	217,24	159,96	152,60	176,66
	NO_X				88,76	94,43	89,95	91,55	93,68	79,25	69,94	62,12	76,29	71,62	56,39	51,44	64,00
	O_3	41,88	40,37														
	PM_{10}	56,11	46,85		32,89	35,50	37,50										
	SO_2	10,07	8,66	9,40	6,87	7,31	7,62	6,25	5,86	7,58	5,52	4,12	5,54	5,56	5,61	6,66	6,09
SANTA CLARA	**CO**	776,98	847,11	903,06	555,51			274,09	332,35	417,65	379,49	317,30	434,24	362,69	221,01	236,23	475,92
	NO_X							49,44	51,63	54,86	47,47	41,44	39,61	36,23	36,01	33,76	37,83
	O_3					50,87	56,42	58,46	54,35	56,04	55,63	57,39	51,03	49,85	55,86	52,41	54,69
	PM_{10}	32,36	42,37	41,28	26,47	25,22	35,82	45,71	49,86	39,96	35,88	25,36	25,32	25,31	23,06	20,86	27,67
TORNEO	**CO**													471,68	401,42	477,10	294,74
	NO_X													78,67	67,67	76,88	84,55
	O_3													39,13	46,44	40,09	41,09
	PM_{10}				23,21	25,10	30,08	27,11	35,67	29,78	22,44	22,47	35,47	28,57	30,27	28,48	37,70
	SO_2													3,67	3,36	3,29	3,24

The pollutants recorded at different measurement stations in Seville increased annually during the 1999–2015 period. The Centro and Torneo stations are closer to the historic centre, as shown in Figure 1.

Given the presence of gypsum ($SO_4Ca \cdot 2H_20$) in more than 80 % of the studied samples, potential sources of SO_2 during the formation of black crusts were evaluated. Emissions data were considered from the Ranilla and Príncipes stations, areas with high levels of traffic, and Torneo, with a medium-high level of traffic, as well as the city centre, with low traffic. Levels of sulphur dioxide (SO_2) in the city centre varied between 1.62 µg/m³ in 2006 and 6.71 µg/m³ in 2004. Meanwhile, over the last four years, sulphur dioxide levels have remained essentially constant. At Torneo station, data are only available for the last four years; this area faces a street with a higher level of traffic than the city centre, and its levels of SO_2 are consistently higher than those found on the street Pajaritos. The remaining stations in high traffic areas have high values of SO_2, up to three times those of the city's centre station, as observed at the Principes station; values two-fold higher are found at the Ranilla station.

Pollutants such as NO_x and CO are highly related to circulating traffic, although no clear relationship was observed with traffic levels. For PM_{10} in the city centre, data have also been reported as part of a monitoring network since 2003, and the levels are similar to those of other areas of the city.

The contribution of the industrial sector to air pollution is low in Seville; industrial areas are few and located far from the historic centre. The low index of industrial activities and the variation in the SO_2 levels as a function of traffic circulation confirms that the main source of ambient sulphur in Seville stems from the operation of motor vehicles, in agreement with the findings by **Fernández et al. [52-53]**. Thus, circulating traffic is the main source of sulphur oxides that cause the formation of black crusts on buildings.

The data in this study demonstrate potential differences in the relationship among levels of pollutants, levels of circulating street traffic, and the presence of black crusts and/or deposits found on samples of the studied church facades (Figure 2). Thus, the risk that historic buildings are exposed to the negative effects of pollution should be further evaluated using a method that can visually and geographically display possible point sources of pollution from traffic circulation, in addition to data on street width, which may affect the dispersion of pollutants.

For this, a risk map was elaborated to visualize the risks to historical buildings stemming from pollution (Figure 6).

This hazard map shows levels of vehicular traffic in Seville, according to the criteria established in the PGOU [41]. Roadways are classified based on the following levels of traffic: structural, the loop around the historic centre with high levels of traffic (hazard factor 5, red); medium (hazard factor 4, orange), characterising the entrance and exit ways of the historic centre; streets limited to public transportation (hazard factor 3, yellow); pedestrian streets with low traffic (hazard factor 1, dark green); and the remaining streets with limited circulation, classified as low traffic (hazard factor 2, light green). This hazard map (Figure 6) suggests that facades facing streets with higher levels of traffic have a greater probability of developing black crusts and deposits.

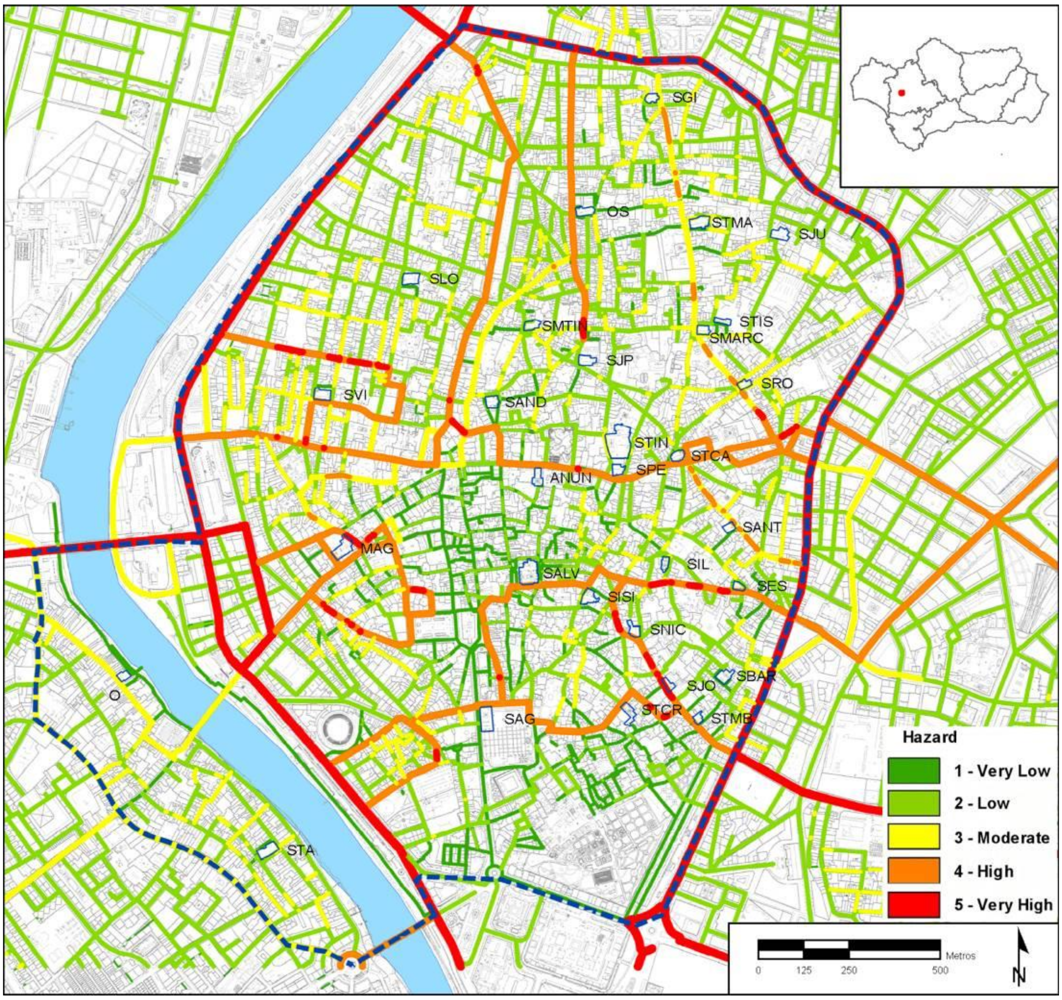

Figure 6. Pollution hazard map due to traffic in the historic centre of Seville (Spain)

The loop, which has very high levels of traffic, is located relatively far from the most emblematic monuments of the city. Several of the studied church facades are located along the entrance and exit ways of the historic centre, which have high levels of traffic, and may continue to be affected, such as Santa Catalina, San

Pedro, Anunciación, San Vicente, Omnium Sanctorum, Salvador, San Isidoro, San Esteban, San Nicolás, San José, Santa María la Blanca, and la Magdalena. Meanwhile, the rest of the facades are located along circulation routes considered to have very low, low or medium hazard.

The hazard map (Figure 6) may be further enhanced by including the effect of streets with widths ≤ 5 m between opposing facades. The close proximity of circulating traffic to facades accelerates their blackening and represents an increased hazard. In the modified hazard map below, street width less than 5 m represents an additional factor and increases risk by one unit. For example, the street San José as well as its extension, the street Santa María la Blanca (Figure 7), are exit routes from the centre where San Jose church is located, which is on a street ≤ 5 m in width. Therefore, hazard increases from high to very high for that facade (Figure 7). This church has a facade sealed with stone that is visibly damaged due to the effects of black crusts/deposits.

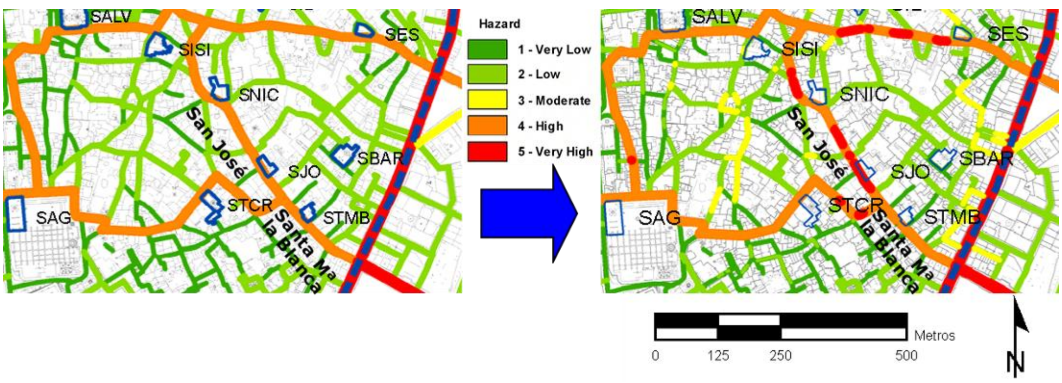

Figura 7. Detail of the traffic hazard map near the streets San José and Santa María la Blanca.

Based on the environmental pollution data for the historic centre of Seville, the concentration of ambient sulphur oxide (SO_2) confirms the influence of circulating vehicles; areas with higher traffic have higher levels of these oxides. Additionally, the appearance of black crusts on the facades of monuments multiplies when they face a street with a high level of traffic, which is similar to the analysed cases from other cities [54-57].

3.3. Digital image analysis of the extent of damage to facades

The degree of blackening of the facades was examined using DIA to further evaluate the methods applied.

The results of this applied methodology allow the identification of the weathering forms and the extent of alteration, including missing parts and the presence of crusts, deposits, or colouration and discolouration; the affected surfaces may then be separated from those without alterations or with repaired mortar. Surfaces with the presence of deposits and/or crusts may be grouped into three categories according to the extent and thickness of the deposits, in addition to the shift of the grayscale histogram (Figure 5).

In Figure 8, the DIA of the facades of the churches Magdalena, Santa Marina, and San Martín is shown; these are located on streets with high, medium, and low levels of traffic, respectively. This analysis reveals the appearance of crusts and/or deposits (yellow, green, and blue colours) on 89 %, 74 %, and 64 % of the analysed surfaces. Over the course of time, all churches exhibit an overall blackening of more than 60 % of their facade as a consequence of the wet and dry deposition of pollutants and airborne particulates, including San Martín, despite its location on a low-traffic street. This result may be due to the cleaning and restoration of the facades of Santa Marina and Magdalena in 1993 and 1991, respectively, whereas the facade of San Martín has not received these efforts. Thus, deposits have accumulated on its facade for a longer period of time.

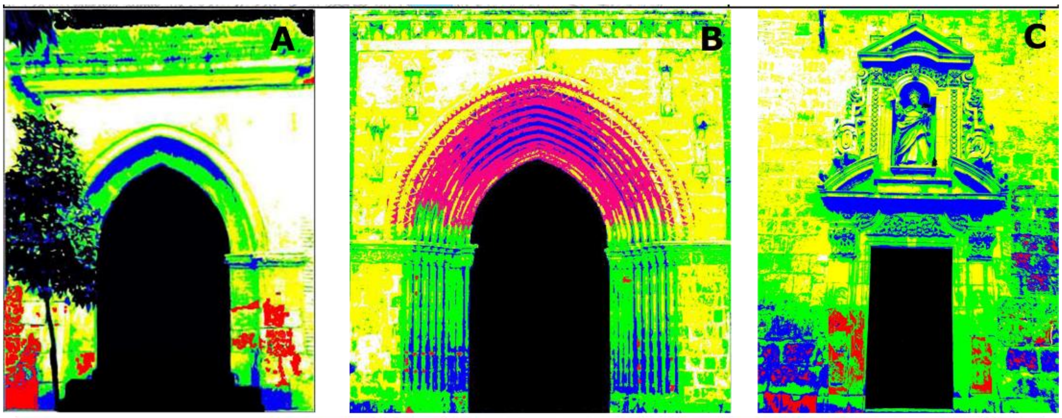

	San Martín	Santa Marina	Magdalena	
Stone and/or repaired mortar	27	10	7	white
Slight deposits	21	39	32	yellow
Medium deposits	30	26	40	green
Thick deposits	13	9	17	blue
Missing part	9	2	4	red
Colouration		14		magenta

Figure 8. A Digital image analysis of the San Martin church facade. B Digital image analysis of the Santa Marina church facade. C Digital image análisis of the Magdalena church facade. Percentage of alteration on facade surface.

The present analysis was applied to a total of 10 churches (13 facades). In Figure 9, the quantification of the extent of alterations may be observed. Churches along roadways with high levels of traffic (San Pedro, Magdalena, Omnium Sanctorum facade 1, Santa Cruz, Santa Catalina, and Anunciación) have more than 80 % of their facades covered with crusts and deposits, whose thickness depends on the time since the most recent restoration, level of traffic, and street width.

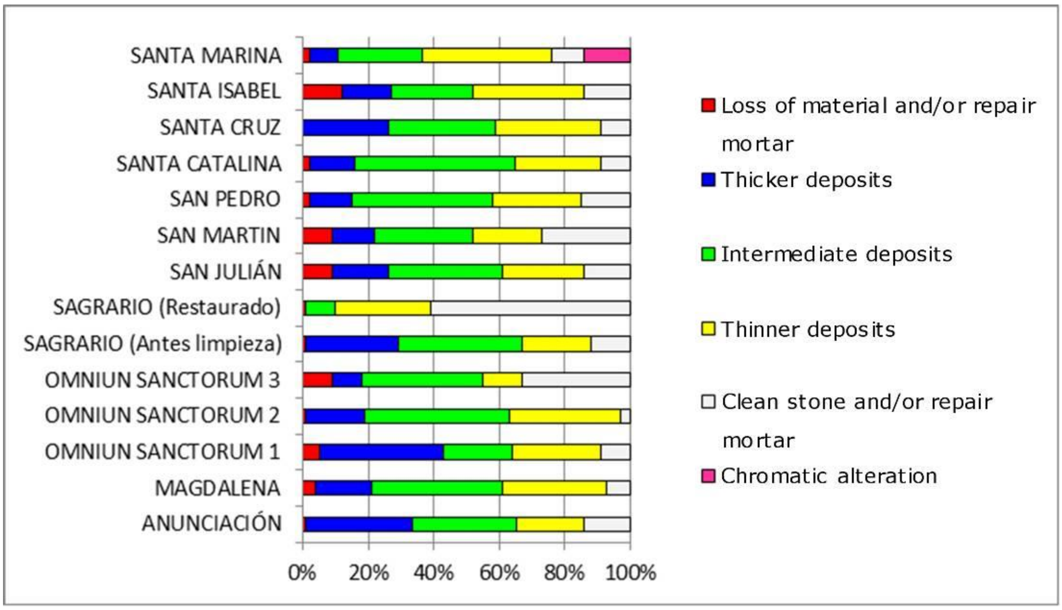

Figure 9. Percentage of alteration on facade surface via digital image analysis.

Facade 2 of Omnium Sanctorum and the Sagrario facade, before its cleaning, presented similarly high values of alteration despite being situated on streets with low traffic. In the case of Omnium Sanctorum, the time since the last restoration, as well as the presence of parking spaces near its entrance until 2013, may be the possible causes. In the case of Sagrario, Constitución Avenue is currently pedestrianised, although it was previously one of the streets with the highest levels of traffic in the city centre and one of the main public transportation routes for buses. These results coincide with recent research performed by Ruffolo et al (2015) that showed that black crusts from the Cathedral of Seville are primarily due to vehicular traffic pollution, where the difference in thickness is due to different exposures to vehicular traffic.

In this study of the city of Seville, several analytical methods were combined to demonstrate that the most extensive and thickest black crusts on buildings are found on streets with higher levels of circulating traffic and on monuments where restorations have not been recent. The alterations to facade surfaces have been extensive because traffic control measures have not been effective or changed within the last 20 years, in spite of the negative effects of pollution.

Regarding preventative measures for the preservation of historic centres, the necessity of introducing improved traffic control measures is clear, which would decrease vehicular access and, in the long-term, favour means of public transportation that do not emit particulate matter. For residents and for loading and unloading vehicles, positive reinforcement measures should be applied to minimise the risk of vehicular traffic.

Furthermore, traffic reorganisation measures are low cost and applicable to any historic centre. The transit of vehicles that emit particulate and gas pollution should be minimised in historic centres; public transportation may be shifted towards tramway systems or the transformation of the fleet towards more efficient vehicles.

DIA allows for the evaluation of the degree of blackening of facades and validates the direct relationship of this phenomenon with circulating traffic. This mode of analysis may also be applicable in other cities.

In addition, DIA may be used to periodically evaluate the responsiveness of traffic control measures in light of the preservation status of cultural heritage.

4. CONCLUSIONES

The integration of GIS and DIA to assess the effects of pollution due to traffic intensity is one analytical methodology that may be used to assess the risk to monuments in historic centres and to further evaluate street width and the higher potential risk of narrow streets, in addition to considering the negative effect of black crusts/deposits. This method may be employed as part of a periodic evaluation of the effects of pollution on the facades of monuments in historic centres.

The results highlight the necessity of reorganising traffic and pedestrianising streets near the monuments of historic centres. These measures may be grounded in the results and methodology of this study. Thus, better decision making in traffic management may be based on the use of geographic information systems for analysis, in addition to more specific measures of preventative control to improve the preservation status of monuments, which may be assessed via DIA.

ACKNOWLEDGEMENTS

This paper has been supported and based on the Methodology developed by two Projects: RIVUPH, an Excellence Project of Junta de Andalucia (code HUM-6775), and Art-Risk, a RETOS project of Ministerio de Economía y Competitividad and Fondo Europeo de Desarrollo Regional (FEDER), (code: BIA2015-64878-R (MINECO/FEDER UE)). Part of the research has been carried out thanks to the grant of Rocío Ortiz from Cei-Patrimonio UN-10.

References

[1] J. Watt, J. Tidblad, V. Kucera, R. Hamilton, The Effects of Air Pollution on Cultural Heritage, Springer, 2009

[2] P. Brimblecombe, Effects of the cultural environment, in: R. Van Grieken, K. Janssens (Eds.), Cultural heritage conservation and environmental impact assessment by non destructive testing and micro-analysis, CRC Press, Leiden, Balkema, 2005, pp. 11–18.

[3] A. Umbría, J. Gervilla, M. Galán, R. Valdés, Caracterización de partículas, Junta de Andalucía, Consejería de Medio Ambiente, 1999.

[4] D. Camuffo, R. Van Grieken, H.J. Busse, G. Sturaro, A. Valentino, A. Bernardi, Environmental monitoring in four European museums, Atmos Environ. 35 (2001) 127–40.

[5] C. Sabbioni, N. Ghedini, A. Bonazza, Organic anions in damage layers on monuments and buildings, Atmos Environ 37 (2003) 1261–9.

[6] A. Bonazza, C. Sabbioni, N. Ghedini, Quantitative data on carbon fractions in interpretation of black crusts and soiling in European built heritage, Atmos Environ 39 (2005) 2607–18.

[7] E. Alonso, L. Martinez, The role of environmental sulfur on degradation of ignimbrites of the Cathedral in Morelia, Mexico, Building and Environment, 38(6) (2003) 861-7.

[8] A. Moropoulou, T. Tsiourva, K. Bisbikou, V. Tsantila, G. Biscontin, G. Longega, Evaluation of cleaning procedures on the facades of the Bank of Greece historical

building in the center of Athens, Building and Environment, 37(7) (2002) 753-60.

[9] I. Ozga, A. Bonazza, S.A. Lyazidi, M. Haddad, A. Ben-Ncer, N. Ghedini, Pollution impact on the ancient ramparts of the Moroccan city Sale, Journal of Cultural Heritage, 14(3) (2013) 25-33.

[10] S.A. Ruffolo, V. Comite, M.F. La Russa, C.M. Belfiore, D. Barca, A. Bonazza, An analysis of the black crusts from the Seville Cathedral: A challenge to deepen the understanding of the relationships among microstructure, microchemical features and pollution sources, Science of the Total Environment, 502 (2015) 157-66.

[11] P. Ortiz, V. Antunez, R. Ortiz, J.M. Martin, M.A. Gomez, A.R. Hortal, Comparative study of pulsed laser cleaning applied to weathered marble surfaces, Applied Surface Science, 283 (2013) 193-201.

[12] Recomendación (97)2 del Comité de Ministros a los Estados Miembros relative a la conservación contínua del Patrimonio Cultural contra el deterioro físico debido a la polución y a factores similares. Comité de Ministros el 4 de Febrero de 1997 en la 583ª reunión de los Delegados de Ministros. Consejo de Europa.

[13] Ley 34/2007 de 15 de noviembre de calidad del aire y protección de la atmósfera. Jefatura de Estado. Boletín Oficial del Estado nº 275 de 16 de noviembre de 2007.

[14] Decreto 239/2011 de 12 de julio por el que se regula la calidad del medio ambiente atmosférico y se crea el Registro de Sistemas de Evaluación de la

Calidad del Aire en Andalucía. Consejería de Medio Ambiente. Boletín Oficial de la Junta de Andalucía Nª 152 de 4 de agosto.

[15] Directiva 2008/50/CE, del Parlamento Europeo y del Consejo, de 21 de mayo de 2008, relativa a la calidad del aire ambiente y a una atmósfera más limpia en Europa. Diario Oficial de la Unión Europea del 11 de junio de 2008.

[16] Plan Nacional de adaptación al cambio climático. Oficina Española de Cambio Climático. Ministerio de Medio Ambiente. Páginas 59. 2008

[17] M. Ford, R. Griffiths, L. Watson, The Sandford Inventory of Earth Buildings constructed using a GIS, Building and Environment, 40(7) (2005) 964-72.

[18] J.A. Gonzalez, M.L.G. Docampo, I.C. Guerrero, The application of new technologies in construction: Inventory and characterisation of rural constructions using the Ikonos satellite image, Building and Environment, 41(2) (2006) 174-83.

[19] M. Indirli, H. Razafindrakoto, F. Romanelli, C. Puglisi, L. Lanzoni, E. Milani, Hazard Evaluation in Valparaiso: the MAR VASTO Project, Pure and Applied Geophysics, 168(3-4) (2011) 543-82.

[20] D.M. Tralli, R.G. Blom, V. Zlotnicki, A. Donnellan, D.L. Evans, D.L., Satellite remote sensing of earthquake, volcano, flood, landslide and coastal inundation hazards, ISPRS J. Photogramm. Remote Sens, 59 (2005) 185–198.

[21] S. Morelli, A. Battistini, F. Catani, Rapid assessment of flood susceptibility in urbanizad rivers using digital terrain data: application to the Arno river case study (Firenze, northern Italy), Appl. Geogr, 54 (2014) 35–53.

[22] F. Cherqui, A. Belmeziti, D. Granger, A. Sourdril, P. Le Gauffre, Assessing urban potencial flooding risk and identifying effective risk-reduction measures, Sci. Total Environ, 514 (2015) 418–425.

[23] O. Unsalan, A.H. Kuzucuoglu, Effects of hazardous pollutants on the walls of Valence Aqueduct (Istanbul) by Raman spectroscopy, SEM-EDX and Geographical Information System, Spectrochimica Acta Part a-Molecular and Biomolecular Spectroscopy, 152 (2016) 572-6.

[24] J. Barriuso, Aplicaciones del proceso digital de imágenes en Arqueología: Experiencias con los sistemas “MIP” y “GEO-JARS” de MICROM, in: Complutum nº 1, 1991, pp. 319-323.

[25] L. Pérez-Barnuevo, R. Castroviejo, E. Berrezueta, Análisis Digital de Imágenes RGB aplicado a la Geometalurgia. Puesta a punto del equipo y su potencial frente a métodos tradicionales, MACLA 11 (2009) 143–144.

[26] D. García del Amo, Determinación de parámetros mineralógicos mediante análisis digital de imagen, Cuadernos Lab. Xeolóxico de Laxe, 25 (2000) 119-122.

[27] M.C. Angel, B. Martínez, N. Prendes, F. Rodríguez, Monuments deterioration evaluation, using digited images. A methodology, Materiales de Construcción, 45(240) (1995) 37-46.

[28] A.R. Gillespie, A.B. Kahle, R.E. Walker, R.E., Color enhancement of highly correlated images. I. Decorrelation and HSI contrast stretches, Remote Sensing of Environment, 20 (1986) 209-235.

[29] R. Mark, E. Billo, Computer-assisted photographic documentation of rock art,

Coalition, 11 (2006) 10-14.

[30] J.M. Vicent García, I. Montero Ruíz, A.L. Rodríguez Alcalde, M.I. Martínez Navarrete, T. Chapa Brunet, Aplicación de la imagen multiespectral al estudio y conservación del arte rupestre postpaleolítico, Trabajos de Prehistoria 53 (1996) 19-35.

[31] A. López, M. Sameño, Aplicación del análisis digital de imagen a los estudios de biodeterioro del Patrimonio Histórico, Revista PH: Instituto Andaluz de Patrimonio Histórico, (1998) 86-91.

[32] F. Zezza, Computerized analysis of stone decay in Monuments, in: Proceedings of the 1ST International Symposium for the Conservation of Monuments in the Mediterranean Basin, Bari, 1989, pp. 163-184.

[33] F. Zezza, Digital image processing of weathered stone in polluted atmosphere, in: Weathering and Air Pollution 1st Course of CUM, Lago di Garda (Portese), 1991, pp. 217-228.

[34] M.A. Vazquez, E. Galan, M.A. Guerrero, P. Ortiz, Digital image processing of weathered stone caused by efflorescences: A tool for mapping and evaluation of stone decay, Construction and Building Materials, 25(4) (2011) 1603-11

[35] M.A. Vazquez, E. Galan, P. Ortiz, R. Ortiz, Digital image analysis and EDX SEM as combined techniques to evaluate salt damp on walls, Construction and Building Materials, 45 (2013) 95-105.

[36] A. Moropoulou, K.C. Labropoulos, E.T. Delegou, M. Karoglou, A. Bakolas, Non-destructive techniques as a tool for the protection of built cultural heritage,

Construction and Building Materials, 48 (2013) 1222-39.

[37] M.A. Rogerio-Candelera, V. Jurado, L. Laiz, C. Saiz-Jimenez, Laboratory and in situ assays of digital image analysis based protocols for biodeteriorated rock and mural paintings recording, Journal of Archaeological Science, 38(10) (2011) 2571-8.

[38] ILLUSTRATED glossary on stone deterioration patterns, ICOMOS-ISCS, 2008, pp. 78.

[39] CNR-ICR NORMAL 3/80 . Materiale lapidei: Campionamento, Istituto Centrale per il Restauro, 1990, pp. 1–6.

[40] REDIAM, Red de Información Ambiental. Junta de Andalucía, 2015. http://www.juntadeandalucia.es/medioambiente/site/rediam

[41] PGOU. Plan General de Ordenación Urbanística de Sevilla, 2006.

[42] A. Casado, Estudio del tráfico y del ruido en el centro histórico de Sevilla, Trabajo Fin de Grado, Facultad de Ciencias Experimentales, Universidad Pablo de Olavide, 2014.

[43] R. Ortiz, P. Ortiz, M.S. Abad, J.M. Martín, A. Gómez, A. Vázquez, Estudio estratigráfico de costrasy depósitos en templos del casco histórico de Sevilla, Revista PH, Instituto Andaluz de Patrimonio Histórico, 2012, 50-61.

[44] Oficina Virtual del Catastro, Sede Electrónica de la Dirección General del Catastro, https://www.sedecatastro.gob.es/

[45] C. Escudero, P. Ortiz, R. Ortiz, J.M. Martín, M.A. Vázquez, M.A. Gómez, Análisis del Estado de Conservación de la Iglesia de Omnium Sanctorum (Sevilla),

Macla, Revista de la Sociedad Española de Mineralogía, 15 (2011) 81–82.

[46] M.L. Ruiz, P. Ortiz, R. Ortiz, J.M. Martín, M.A. Vázquez, M.A. Gómez, Estado de Conservación de la Fachada de la Iglesia de Santa Cruz (Sevilla), Macla, Revista de la Sociedad Española de Mineralogía, 15 (2011) 185–186.

[47] F. Zezza, Digital Image Processing in Weathering Damage Analysis and Recovery Treatments Monitoring, Digital Heritage, 6436 (2010) 71-84.

[48] F. Colao, R. Fantoni, P. Ortiz, M.A. Vázquez, J.M. Martín, R. Ortiz, N. Idris. Quarry Identification of Historical Building Materials by Means of Laser Induced Breakdown Spectroscopy, X-Ray Fluorescence And Chemometric Analysis. Spectrochimica Acta Part B 65 (2010) 688–694.

[49] P. Ortiz, M.A. Vázquez, J.M. Martín, R. Ortiz, M.S. Abad, M.A. Guerrero, Estado de Alteración de la Fachada Principal de La Iglesia de Santa Catalina (Sevilla), Macla, Revista de la Sociedad Española de Mineralogía, 11 (2009) 139-140.

[50] P. Bromblet, V. Verges-Belmin, L`élimination del sulfates sur la statuaire calcaire de plein air: une habitude discutable, Le dessalement des Materiaux Poreux. Jornées d`études de la SFIIC, 1996, pp. 55-64.

[51] M.A. Guerrero, Diagnóstico del Estado de Alteración de la Piedra del Palacio Consistorial de Sevilla. Causas y Mecanismos. Tesis. Universidad de Sevilla. 1990, pp. 265.

[52] A.J. Fernàndez, M. Ternero, F.J. Barragàn, J.C. Jimènez, An approach to characterization of sources of urban airborne particles through heavy metal

speciation, Chemosphere Global Change Sci, 2(2) (2000) 123–36.

[53] A.J. Fernández, M. Ternero, Study of traffic pollution by metals in Seville (Spain) by physical and chemical speciation methods, Anal. Bioanal. Chem, 379 (2004) 684–699.

[54] R.A. Lefevre, A. Jonescu, P. Ausset. (2005) Modeling the calcareous stone sulphation in polluted atmosphere after exposure in the field, in: R. Priklyl, B. Smith (eds.) Natural Stone Decay. London: Geological Society, 2005

[55] T. Thi Ngox Lan, N. Thi Phuong Thoa, R. Nishimurab, New model for the sulphation of marble by dry deposition Sheltered marble-the indicator of air pollution by sulphur dioxide, Atmospheric Environment, 39 (2005) 913-920.

[56] D. Camuffo, E. PAGAN, M. MONTE, Modeling the penetration of SO_2 within the pores of calcareous stones and the concentration of gypsum in the near surface layer, in: R. Fort, M. Álvarez de Buergo, M. Gómez-Heras (eds.) Heritage, weathering and conservation (Madrid, 21 al 24 june 2006). Londres: Taylor & Francis, 2006, pp. 435-440

[57] C.M. Grossi, P. Brimblecombe, Sulfate and carbon compounds in black crusts from the Cathedral of Milan and Tower of London, in: R. Fort, M. Álvarez de Buergo, M. Gómez-Heras (eds.) Heritage, weathering and conservation (Madrid, 21 al 24 june 2006). Londres: Taylor & Francis, 2006, pp. 441-446.